JCAMECH

Vol. 49, No. 1, June 2018, pp 86-101
DOI: 10.22059/jcamech.2018.248906.223

Free vibration analysis of nanoplates made of functionally graded materials based on nonlocal elasticity theory using finite element method

A. Zargaripoor[a], A. Daneshmehr[a,], I. Isaac Hosseini[a] ,A. Rajabpoor[a]*

[a] *School of Mechanical Engineering, College of Engineering, University of Tehran, Tehran, Iran*

ARTICLE INFO

Article history:
Received: *01 January 2018*
Accepted: *30 January 2018*
Available online

Keywords:
FEM
HSDT Plate
Free Vibration
FG Nanoplate
Nonlocal Theory

ABSTRACT

In this paper, an analysis of free vibration in functionally graded nanoplate is presented. Third-order shear deformation plate theory is used to reach more accuracy in results. Small-scale effects are investigated using Eringen`s nonlocal theory. The governing equations of motion are obtained by Hamilton`s principle. It is assumed that the properties of nanoplates vary through their thicknesses according to a volume fraction power law distribution. The finite element method (FEM) is presented to model the functionally graded nanoplate and solve mathematical equations accurately. The finite element formulation for HSDT nanoplate is also presented. Natural frequencies of FG nanoplate with various boundary conditions are compared with available results in the literature. At the end some numerical results are presented to evaluate the influence of different parameters, such as power law index, nonlocal parameter, aspect ratio and aspect of length to thickness of nanoplate. In addition, all combinations of simply supported and clamped boundary conditions are considered.

1. Introduction

As powerful engines, turbines, reactors, and other machines have been developed in recent years in aerospace industries, the need for materials with high thermal and mechanical resistance has been identified. Functionally graded materials (FGMs) are among the materials that exhibit different properties in different regions due to gradual changes in their chemical compositions or due to changes in distribution, orientation, or phase of reinforcement in one or more dimensions. This gradual change in structure and properties has caused the application of such materials to spread, particularly in cases where different properties are needed in different regions. Since multilayer composites are composed of two dissimilar materials next to one another, the layers may tend to get isolated.

Cracks are most probably formed in the mediate region between the two materials, and spread into the weaker part. Furthermore, residual stress may occur in the block due to different temperature coefficients. These problems can indicate that the common multilayer composites need to be replaced by functionally graded materials, where the properties gradually change in microscopic scale linearly through the thickness. A common type of FGM includes a continuous combination of a ceramic and a metal. The change from pure metal to pure ceramic is incremental and continuous such that one surface is made of pure ceramic and the other of pure metal. The mechanical properties also change continuously through the thickness based on the compound type.

The free vibrations of functionally graded materials have been studied widely in recent years. Aksencer and Aydogdu [1] studied buckling and vibration of nanoplates using nonlocal elasticity theory. The Navier type solution is used for simply supported plates and the Levy type method is used for plates with two opposite edges simply supported and remaining edges arbitrarily supported. Ansari et al. [2] developed a nonlocal plate model which accounts for the small-scale effects to study the vibrational characteristics of multi-layered graphene sheets with different boundary conditions embedded in an elastic medium. Hosseini, Hashemi and Samaei [3] proposed an analytical solution for the buckling analysis of rectangular nanoplates. Narendar [4] presented a buckling analysis of isotropic nanoplates using the two-variable refined plate theory and nonlocal small-scale effects. Daneshmehr et al. [5] investigated the free vibration behavior of the nanoplate made of functionally graded materials with small-scale effects. The generalized differential quadrature method (GDQM) was used to solve the governing equations for various boundary conditions to obtain

* Corresponding Author. . Tel.: +98 21 88005677; Fax: +98 21 88013029
Email Address: daneshmehr@ut.ac.ir

the nonlinear natural frequencies of FG nanoplates. Bakhsheshy and Khorshidi [6] presented the free vibration analysis of functionaly graded rectangular nanoplates in thermal environments. The modified coupled stress theory, based on the first order shear deformation theory, was used to obtain the natural frequencies of the nanoplate. Hosseini, Hashemi et al. [7] presented analytical solutions for free vibration analysis of moderately thick rectangular plates, which are composed of functionally graded materials and supported by either Winkler or Pasternak elastic foundations. Zare et al.[8] analyzed the natural frequencies of a functionally graded nanoplate for different combinations of boundary conditions. Natarajan et al. investigated the size-dependent linear free flexural vibration behavior of functionally graded nanoplates using the iso-geometric-based finite element method. Bounouara et al.[9] presented a zeroth-order shear deformation theory for free vibration analysis of functionally graded nanoscale plates resting on elastic foundations. Salehipour et al. [10] developed a model for static state and vibration of functionally graded micro/nano plates based on modified couple stress and three-dimensional elasticity theories. Belkorissat et al. [11] presented a new nonlocal hyperbolic refined plate model for free vibration properties of functionally graded plates. Ansari et al. [12] studied the buckling and vibration responses of nanoplates made of functionally graded materials subjected to thermal loading in a perbuckling domain while considering the effect of surface stress. Hosseini and Jamalpoor [13] studied the dynamic characteristics of a double-FGM viscoelastic nanoplates system subjected to temperature change while also considering surface effects based on the nonlocal elasticity theory of Eringen. Ansari et al. [14] presented a three-dimensional nonlocal bending and vibration analysis of functionally graded nanoplates using a novel numerical solution method which is called variational differential quadrature (VDQ) due to its numerical essence and the framework of implementation. Aghababaei and Reddy[15] studied the vibration of isotropic rectangular nanoplate using the nonlocal elasticity theories and the third-order shear deformation theory. Bouiadjra et al. [16] investigated nonlinear behavior of functionally graded material plates under thermal loads using an efficient sinusoidal shear deformation theory. Nguyen et al. [17] proposed an efficient computational approach based on refined plate theory (RPT) which included the thickness stretching effect, namely quasi-3D theory, in conjunction with iso-geometric formulation (IGA) for the size-dependent bending, free vibration and buckling analysis of functionally graded nanoplate structures. Daneshmehr et al.[18] presented a nonlocal higher order plate theory for stability analysis of nanoplates subjected to biaxial in plane loadings. The generalized differential quadrature (GDQ) method was implemented to resolve size-dependent buckling analysis according to higher-order shear deformation plate theories, where highly coupled equations exist for various boundary conditions of rectangular plates. Ghorbanpour, Arani et al. [19] investigated modeling and vibration analysis of carbon nanotubes/fiber/polymer composite microplates. Goodarzi et al. [20] studied the free vibration behavior of nanoscale FG rectangular plates within the framework of the refined plate theory (RPT) and small-scale effects were taken into account. Raissi et al. [21] used layerwise theory along with first-, second- and third-order shear deformation theories to determine the stress distribution in a simply supported square sandwich plate subjected to a uniformly distributed load. Mergen et al. [22] investigated the size-dependent nonlinear oscillation characteristics of a functionally graded microplate numerically. Baghani et al. [23] studied the effects of magnetic field, surface energy and compressive axial load on the dynamic and the stability behavior of the nanobeam. Ghayesh et al. [24] investigated the size-dependent oscillations of a third-order shear-deformable functionally graded microbeam taking into account all the longitudinal and transverse displacements and inertia as well as the rotation and rotary inertia. Kordani et al. [25] presented a numerical procedure for the free and forced vibration of a piezoelectric nanowire under thermos-electro-mechanical loads based on the nonlocal elasticity theory within the framework of Timoshenko beam theory. Farajipour and Rastgoo [26] developed a modified beam model to investigate the effect of carbon nanotubes on the buckling of microtubule bundles in living cell. Hosseini et al. [27] studied stress distribution in a single-walled carbon nanotube under internal pressure with various chirality. Hosseini et al. [28] presented the stress analysis of ratating nano-disk of functionally graded materials with nonlinearly varying thickness based on strain gradient theory. Zamani Nejad et al. [29] used a semi-analytical iterative method as one of the newest analytical methods for the elastic analysis of thick-walled spherical pressure vessels made of functionally graded materials subjected to internal pressure. In other work, Zamani Nejad and Hadi [30] formulated the problem of the static bending of Euler-Bernoulli nano-beams made of bi-directional functionally graded material with small scale effects. Also, Zamani Nejad and Hadi [31] investigated the free vibration analysis of Euler-Bernoulli nano-beams made of bi-directional functionally graded material with small scale effects. Zamani Nejad et al. [32] presented consistent couple-stress theory for free vibration analysis of Euler-Bernoulli nano-beams made of arbitrary bi-directional functionally graded materials. Also, Zamani Nejad et al. [33] presented buckling analysis of the nano-beams made of two-directional functionally graded materials with small scale effects based on nonlocal elasticity theory. In other work, Zamani Nejad et al. [34] presented an exact closed-form analytical solution for elasto-plastic deformations and stresses in a rotating disk made of functionally graded materials in which the elasto-perfectly-plastic material model is employed. Shishesaz et al. [35] studied the thermoelastic behavior of a functionally graded nanodisk based on the strain gradient theory. Hadi et al. [36] presented buckling analysis of FGM Euler-Bernoulli nano-beams with 3D-varying properties based on consistent couple-stress theory. Zamani Nejad et al. [37] discussed some critical issues and problems in the development of thick shells made from functionally graded piezoelectric material. Hadi et al. [38] presented an investigation on the free vibration of three-directional functionally graded material Euler-Bernoulli nano-beam, with small scale effects.

In this study, free vibration of functionally graded nanoplate is presented. Higher-order shear deformation plate theory is considered [39]. According to the literature review presented above, in this study, the finite element method has been used for analyzing the vibration of FG Nanoplates for the first time. In this study, for the first time, the formulation of the Finite Element Method for the *third-order shear deformation* plate theory is presented. Natural frequencies for all different combinations of boundary conditions are presented for simply supported and clamped for different modes. For applying small-size effects, nonlocal theory is used and for various nonlocal parameters, the natural frequencies of nanoplate calculated. The results of the calculations are provided in the conclusion.

2. Mathematical formulation

2.1 Geometrical configuration

In Figure 1, a functionally graded rectangular nanoplate of length L_1, width L_2 and height h is shown. Cartesian coordinates (x, y, z) is considered.

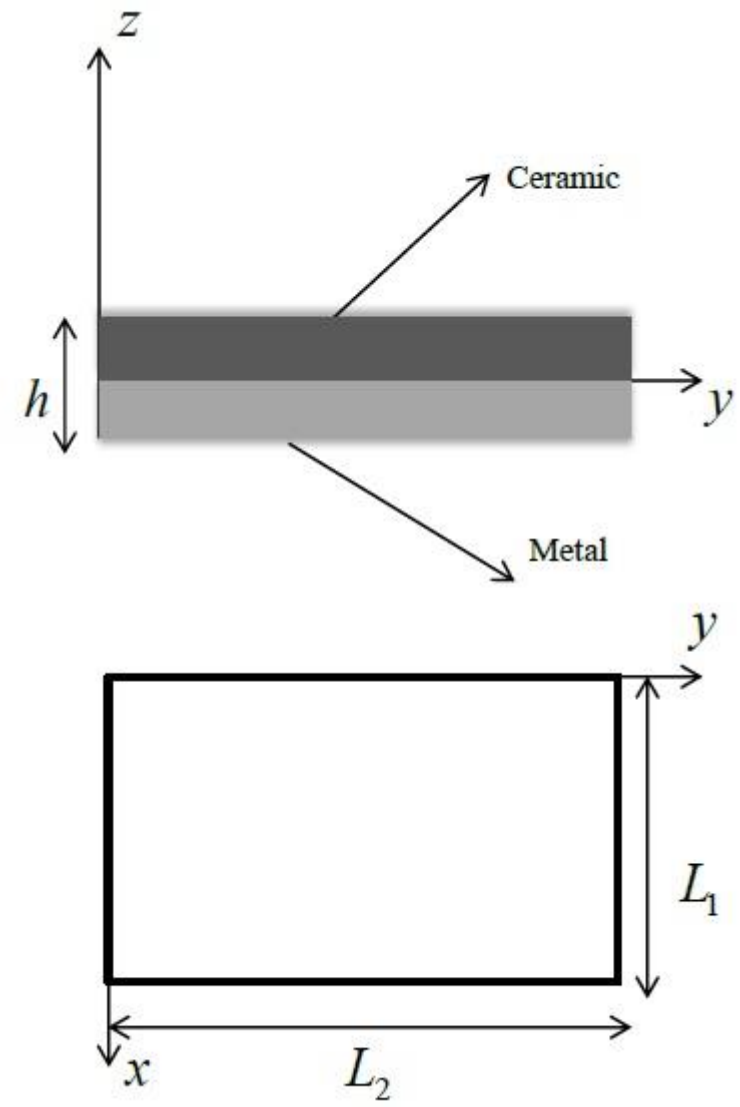

Fig 1. Geometry of functionally graded rectangular nanoplate

2.2 Material properties

Functionally graded plate consists of two metal and ceramic parts which are integrated in such a way that material properties are continuously and gradually changed along with plate thickness from purely metal properties in the bottom surface of plate $(z = -\frac{h}{2})$ to purely ceramic properties in the top of the plate $(z = +\frac{h}{2})$. Assuming that the distribution of the material properties through thickness follows the power law, the following equation could be written.

$$P = P_m V_m + P_c V_c \tag{1}$$

Where P_m and P_c, respectively, show metal and ceramic properties, and V_m and V_c show the volume fraction of the metal and ceramic parts in the bottom and top surfaces of the plate. By using the power distribution law, the volume fraction of the ceramic part is noted for each point of plate thickness in Eq. (2) and (3). [40]

$$V_c = (\frac{z}{h} + \frac{1}{2})^n \tag{2}$$

$$V_m + V_c = 1 \tag{3}$$

Where *n* indicates the volume fraction index of the ceramic and the distribution of the ceramic part is noted along with plate. So according to the above equation, the properties of the graded

materials is a function of E, Young modulus and unit mass of volume ρ, along with the plate thickness as shown in the following equations.

$$E(z) = (E_c - E_m)V_c + E_m \tag{4}$$

$$\rho(z) = (\rho_c - \rho_m)V_c + \rho_m \tag{5}$$

2.3 Non-local elasticity theory

Nonlocal elasticity theory, which was introduced by Eringen [41], is one of the unconventional contemporary theories in that the effects of small scales are applied in the characteristic equations of this theory. In nonlocal theory, the stress tensor at the point x of a physical environment Ω is connected to the strain tensor ε in the whole of the environment by an integral equation. In other words, the constitutive law of nonlocal theory is

$$\sigma(x) = \iiint \alpha\left(|x' - x|, \tau\right) C\varepsilon(x')dv \tag{6}$$

Element $\alpha\left(|x' - x|, \tau\right)$ is called the nonlocal modulus and acts as a weight function in this equation. $|x' - x|$ is the distance between the local point and the nonlocal point. C is a fourth-order tensor which exists in classical theory, too. τ is related to the internal length scale $(\bar{a})$ and outer length scale (l) as

$$\tau = \frac{e_0 \bar{a}}{l} = \sqrt{\frac{\mu}{l^2}} \tag{7}$$

where e_0 is a physical parameter that has been identified by experimental results, and the parameter $\mu = (e_0 \bar{a})^2$ is called the small-size parameter.

At last, the form of the structural equation of non-localized elastic theory is as follows.

$$(1 - \mu\nabla^2)\sigma = C : \varepsilon \tag{8}$$

It should be mentioned, when the body is not small, the small-size parameter is small, and the nonlocal constitutive parameter converges to classical theory.

2.4 The equations of motion

To achieve the equations of motion of thick plate, displacement fields of third-order theory in Cartesian coordinates were used. [39]

$$u(x,y,z,t) = u_0(x,y,t) + z\phi_x(x,y,t) - \frac{4z^3}{3h^2}\left(\phi_x + \frac{\partial w_0}{\partial x}\right) \tag{9}$$

$$v(x,y,z,t) = v_0(x,y,t) + z\phi_y(x,y,t) - \frac{4z^3}{3h^2}\left(\phi_y + \frac{\partial w_0}{\partial y}\right) \tag{10}$$

$$w(x,y,z,t) = w_0(x,y,t) \tag{11}$$

Where u, v and w are the displacements of each point and u_0, v_0 and w_0 are the displacement amounts in the middle sheet in the directions x, y and z, respectively. Also ϕ_x and ϕ_y, respectively, show normal rotation perpendicular to the middle of the plate around y and x axes. By using the displacement fields discussed earlier, the strain equation could be written as follows:

$$\varepsilon_{xx} = \frac{\partial u_0(x,y,t)}{\partial x} + z\frac{\partial \phi_x(x,y,t)}{\partial x} - C_1 z^3\left(\frac{\partial \phi_x}{\partial x} + \frac{\partial^2 w_0}{\partial x^2}\right) \tag{12}$$

$$\varepsilon_{yy} = \frac{\partial v_0(x,y,t)}{\partial y} + z\frac{\partial \phi_y(x,y,t)}{\partial y} - C_1 z^3\left(\frac{\partial \phi_y}{\partial y} + \frac{\partial^2 w_0}{\partial y^2}\right) \tag{13}$$

$$\varepsilon_{zz} = 0 \tag{14}$$

$$\varepsilon_{xy} = \frac{1}{2}\left(\frac{\partial u_0(x,y,t)}{\partial y} + \frac{\partial v_0(x,y,t)}{\partial x}\right) + z\left(\frac{\partial \phi_x(x,y,t)}{\partial y} + \frac{\partial \phi_y(x,y,t)}{\partial x}\right) - C_1 z^3\left(\frac{\partial \phi_x}{\partial y} + 2\times\frac{\partial^2 w_0}{\partial x\,\partial y} + \frac{\partial \phi_y}{\partial x}\right) \tag{15}$$

$$\varepsilon_{xz} = \frac{1}{2}(1 - C_2 z^2)\left(\phi_x + \frac{\partial w_0(x,y,t)}{\partial x}\right) \tag{16}$$

$$\varepsilon_{yz} = \frac{1}{2}(1 - C_2 z^2)\left(\phi_y + \frac{\partial w_0(x,y,t)}{\partial y}\right) \tag{17}$$

Where $C_1 = \frac{4}{3h^2}$ and $C_2 = 3\times C_1$.

The stress-strain relations for the plane stress problem are defined as:

$$L\begin{Bmatrix}\sigma_{xx}\\ \sigma_{yy}\\ \sigma_{xy}\end{Bmatrix} = \begin{bmatrix}Q_{11} & Q_{12} & 0\\ Q_{21} & Q_{22} & 0\\ 0 & 0 & Q_{66}\end{bmatrix}\begin{Bmatrix}\varepsilon_{xx}\\ \varepsilon_{yy}\\ \varepsilon_{xy}\end{Bmatrix} \tag{18}$$

$$L\begin{Bmatrix}\sigma_{xz}\\ \sigma_{yz}\end{Bmatrix} = Q_{66}\begin{Bmatrix}\varepsilon_{xz}\\ \varepsilon_{yz}\end{Bmatrix} \tag{19}$$

where $L = 1 - \mu\nabla^2$ and Q_{ij} are the coefficients of stiffness matrix and defined as follows:

$$Q_{11} = Q_{22} = \frac{E}{1-\nu^2} \tag{20}$$

$$Q_{12} = Q_{21} = \frac{E\nu}{1-\nu^2} \tag{21}$$

$$Q_{66} = \frac{E}{2(1+\nu)} \tag{22}$$

By using displacement field in the Hamilton principle, motion equations based on forces and moments are derived as follows [15]:

$$\delta u_0 : \frac{\partial N_{xx}}{\partial x} + \frac{\partial N_{xy}}{\partial y} = L\left(m_0 \frac{\partial^2 u_0}{\partial t^2} + m_1 \frac{\partial^2 \phi_x}{\partial t^2} - c_1 m_3 \frac{\partial^2 \phi_x}{\partial t^2} - c_1 m_3 \frac{\partial^3 w_0}{\partial t^2 \partial x} \right) \tag{23}$$

$$\delta v_0 : \frac{\partial N_{yy}}{\partial y} + \frac{\partial N_{xy}}{\partial x} = L\left(m_0 \frac{\partial^2 v_0}{\partial t^2} + m_1 \frac{\partial^2 \phi_y}{\partial t^2} - c_1 m_3 \frac{\partial^2 \phi_y}{\partial t^2} - c_1 m_3 \frac{\partial^3 w_0}{\partial t^2 \partial y} \right) \tag{24}$$

$$\delta w_0 : c_1 \frac{\partial^2 P_{xx}}{\partial x^2} + 2c_1 \frac{\partial^2 P_{xy}}{\partial x \partial y} + c_1 \frac{\partial^2 P_{yy}}{\partial y^2} + \frac{\partial \bar{Q}_x}{\partial x} + \frac{\partial \bar{Q}_y}{\partial y} = L\left(\begin{array}{l} m_0 \frac{\partial^2 w_0}{\partial t^2} + \left(c_1 m_4 - c_1^2 m_6\right)\left(\frac{\partial^3 \phi_x}{\partial t^2 \partial x} + \frac{\partial^3 \phi_y}{\partial t^2 \partial y} \right) \\ -c_1^2 m_6 \left(\frac{\partial^4 w_0}{\partial t^2 \partial x^2} + \frac{\partial^4 w_0}{\partial t^2 \partial y^2} \right) + c_1 m_3 \left(\frac{\partial^3 u_0}{\partial t^2 \partial x} + \frac{\partial^3 v_0}{\partial t^2 \partial y} \right) \end{array} \right) \tag{25}$$

$$\delta \phi_x : \frac{\partial \bar{M}_{xx}}{\partial x} + \frac{\partial \bar{M}_{xy}}{\partial y} + \bar{Q}_x = L\left(\begin{array}{l} \left(m_1 - c_1 m_3\right)\frac{\partial^2 u_0}{\partial t^2} + \left(m_2 - 2c_1 m_4 + c_1^2 m_6\right)\frac{\partial^2 \phi_x}{\partial t^2} \\ + \left(c_1 m_4 - c_1^2 m_6\right)\frac{\partial^2 w}{\partial t^2 \partial x} \end{array} \right) \tag{26}$$

$$\delta \phi_y : \frac{\partial \bar{M}_{xy}}{\partial x} + \frac{\partial \bar{M}_{yy}}{\partial y} + \bar{Q}_y = L\left(\begin{array}{l} \left(m_1 - c_1 m_3\right)\frac{\partial^2 v_0}{\partial t^2} \left(m_2 - 2c_1 m_4 + c_1^2 m_6\right)\frac{\partial^2 \phi_y}{\partial t^2} \\ + \left(c_1 m_4 - c_1^2 m_6\right)\frac{\partial^2 w}{\partial t^2 \partial y} \end{array} \right) \tag{27}$$

Where stress resultants in elastic plate are defined as follows:

$$N_{\alpha\beta} = \int_{-h/2}^{h/2} \sigma_{\alpha\beta} dz \quad \text{Force resultants} \tag{28}$$

$$M_{\alpha\beta} = \int_{-h/2}^{h/2} \sigma_{\alpha\beta} z dz \quad \text{Moment resultants} \tag{29}$$

$$P_{\alpha\beta} = \int_{-h/2}^{h/2} \sigma_{\alpha\beta} z^3 dz \quad \text{Higher-order moment resultants} \tag{30}$$

$$Q_{\alpha} = \int_{-h/2}^{h/2} \sigma_{\alpha z} dz \quad \text{Transverse force resultants} \tag{31}$$

$$R_{\alpha} = \int_{-h/2}^{h/2} \sigma_{\alpha z} z^2 dz \quad \text{Transverse higher-order force resultants} \tag{32}$$

$\bar{M}$ and $\bar{Q}$ are

$$\bar{M}_{\alpha\beta} = M_{\alpha\beta} - c_1 P_{\alpha\beta} \tag{33}$$

$$\bar{Q}_{\alpha} = Q_{\alpha} - c_2 R_{\alpha} \tag{34}$$

And components of m are

$$\begin{Bmatrix} m_0 \\ m_1 \\ m_2 \\ m_3 \\ m_4 \\ m_5 \\ m_6 \end{Bmatrix} = \int_{-h/2}^{h/2} \begin{Bmatrix} z^0 \\ z^1 \\ z^2 \\ z^3 \\ z^4 \\ z^5 \\ z^6 \end{Bmatrix} \rho(z) dz \tag{35}$$

Boundary conditions for the two kinds of boundaries are:

Simply supported boundary condition:

$$\begin{aligned} &u_0 = v_0 = w_0 = \phi_y = \bar{M}_{xx} = P_{xx} = 0 \rightarrow x = 0, a \\ &u_0 = v_0 = w_0 = \phi_x = \bar{M}_{yy} = P_{yy} = 0 \rightarrow y = 0, b \end{aligned} \tag{36}$$

Clamped boundary condition:

$$\begin{aligned} &u_0 = v_0 = w_0 = \phi_x = \phi_y = \frac{\partial w_0}{\partial x} = 0 \rightarrow x = 0, a \\ &u_0 = v_0 = w_0 = \phi_x = \phi_y = \frac{\partial w_0}{\partial y} = 0 \rightarrow y = 0, b \end{aligned} \tag{37}$$

3. Solution method

3.1 Finite element method

In this section, a system of equations is solved simultaneously with the finite element method (FEM). At first we separate time and spatial dependencies as follows:

$$\begin{cases} u(x,y,t)=\sum_{i=1}^{4}\bar{u}_i(t)\psi_i^{(1)}u(x,y) \\ v(x,y,t)=\sum_{i=1}^{4}\bar{v}_i(t)\psi_i^{(1)}(x,y) \\ w(x,y,t)=\sum_{i=1}^{12}w_i(t)\psi_i^{(2)}(x,y) \\ \varphi_x(x,y,t)=\sum_{i=1}^{4}\varphi_{xi}(t)\psi_i^{(3)}(x,y) \\ \varphi_y(x,y,t)=\sum_{i=1}^{4}\varphi_{yi}(t)\psi_i^{(3)}(x,y) \end{cases} \quad (38)$$

For the deflection along the z-axis, w, second polynomial interpolation functions (Equation (39)) are chosen, and for other variables, first polynomial interpolation functions (Equation (40)), are chosen, due to the degree of derivations in the equations. These choices are made to prevent shear locking.[42]

$$\begin{Bmatrix} \psi_1^{(2)} \\ \psi_2^{(2)} \\ \psi_3^{(2)} \\ \psi_4^{(2)} \\ \psi_5^{(2)} \\ \psi_6^{(2)} \\ \psi_7^{(2)} \\ \psi_8^{(2)} \\ \psi_9^{(2)} \\ \psi_{10}^{(2)} \\ \psi_{11}^{(2)} \\ \psi_{12}^{(2)} \end{Bmatrix} = \begin{Bmatrix} \frac{1}{8}(1-\zeta)\times(1-\eta)\times(2-\zeta-\eta-\zeta^2-\eta^2) \\ \frac{1}{8}(1+\zeta)\times(1-\eta)\times(2+\zeta-\eta-\zeta^2-\eta^2) \\ \frac{1}{8}(1+\zeta)\times(1+\eta)\times(2+\zeta+\eta-\zeta^2-\eta^2) \\ \frac{1}{8}(1-\zeta)\times(1+\eta)\times(2-\zeta+\eta-\zeta^2-\eta^2) \\ \frac{1}{8}(1+\zeta)\times(1-\eta)\times(1-\zeta)^2 \\ \frac{1}{8}(1-\zeta)\times(1-\eta)\times(1+\zeta)^2 \\ \frac{1}{8}(1+\zeta)\times(1+\eta)\times(1-\zeta)^2 \\ \frac{1}{8}(1-\zeta)\times(1+\eta)\times(1+\zeta)^2 \\ \frac{1}{8}(1-\zeta)\times(1+\eta)\times(1-\eta)^2 \\ \frac{1}{8}(1+\zeta)\times(1+\eta)\times(1-\eta)^2 \\ \frac{1}{8}(1+\zeta)\times(1-\eta)\times(1+\eta)^2 \\ \frac{1}{8}(1-\zeta)\times(1-\eta)\times(1-\eta)^2 \end{Bmatrix} \quad (39)$$

$$\begin{Bmatrix} \psi_1^{(1)} \\ \psi_2^{(1)} \\ \psi_3^{(1)} \\ \psi_4^{(1)} \end{Bmatrix} = \begin{Bmatrix} \psi_1^{(3)} \\ \psi_2^{(3)} \\ \psi_3^{(3)} \\ \psi_4^{(3)} \end{Bmatrix} = \begin{Bmatrix} \frac{1}{4}(1-\zeta)(1-\eta) \\ \frac{1}{4}(1+\zeta)(1-\eta) \\ \frac{1}{4}(1+\zeta)(1+\eta) \\ \frac{1}{4}(1-\zeta)(1+\eta) \end{Bmatrix} \quad (40)$$

Using the Galerkin method, equations (17) to (21) are multiplied in $\psi^{(1)}$, $\psi^{(2)}$ and $\psi^{(3)}$ and the integral is taken through the thickness of the plate. By using integration by parts and arranging the results, the matrices of stiffness and mass are as follows:

$$K^e = \begin{bmatrix} [k_{11}]_{4\times4} & [k_{12}]_{4\times4} & [k_{13}]_{4\times12} & [k_{14}]_{4\times4} & [k_{15}]_{4\times4} \\ [k_{21}]_{4\times4} & [k_{22}]_{4\times4} & [k_{23}]_{4\times12} & [k_{24}]_{4\times4} & [k_{24}]_{4\times4} \\ [k_{31}]_{12\times4} & [k_{32}]_{12\times4} & [k_{33}]_{12\times12} & [k_{34}]_{12\times4} & [k_{35}]_{12\times4} \\ [k_{41}]_{4\times4} & [k_{42}]_{4\times4} & [k_{43}]_{4\times12} & [k_{44}]_{4\times4} & [k_{45}]_{4\times4} \\ [k_{51}]_{4\times4} & [k_{52}]_{4\times4} & [k_{53}]_{4\times12} & [k_{54}]_{4\times4} & [k_{55}]_{4\times4} \end{bmatrix} \quad (41)$$

$$M^e = \begin{bmatrix} [m_{11}]_{4\times4} & [m_{12}]_{4\times4} & [m_{13}]_{4\times12} & [m_{14}]_{4\times4} & [m_{15}]_{4\times4} \\ [m_{21}]_{4\times4} & [m_{22}]_{4\times4} & [m_{23}]_{4\times12} & [m_{24}]_{4\times4} & [m_{24}]_{4\times4} \\ [m_{31}]_{12\times4} & [m_{32}]_{12\times4} & [m_{33}]_{12\times12} & [m_{34}]_{12\times4} & [m_{35}]_{12\times4} \\ [m_{41}]_{4\times4} & [m_{42}]_{4\times4} & [m_{43}]_{4\times12} & [m_{44}]_{4\times4} & [m_{45}]_{4\times4} \\ [m_{51}]_{4\times4} & [m_{52}]_{4\times4} & [m_{53}]_{4\times12} & [m_{54}]_{4\times4} & [m_{55}]_{4\times4} \end{bmatrix} \quad (42)$$

Each component of the above matrices and the vector is presented in Appendix A.

4. Results and discussion

Here, free vibration analysis of FG nanoplates based on the third-order shear deformation plate theory is studied and numerical results are achieved for different boundary conditions by using the finite element method. For the validation of results, the natural frequencies of the nanoplates are compared with the results of Aghababaei and Reddy's study[15]. Also the values of the dimensionless frequencies for FG rectangular nanoplates are compared with Ref [43]. In addition the influence of different parameters, such as nonlocal parameter (μ), aspect ratio ($\eta=\frac{a}{b}$) and aspect of length to thickness ($\delta=\frac{h}{a}$) of nanoplate are assessed.

The values of material properties for FGM nanoplates are listed in table 1.Also, the dimensionless frequency and frequency ratio is defined as follow:

$$\bar{\omega}=\omega h\sqrt{\rho_c/G_c} \quad (43)$$

$$Fr=\frac{\overline{\omega_{NL}}}{\overline{\omega_L}} \quad (44)$$

In which $\bar{\omega}_L$ is dimensionless frequency when $\mu=0$.

Table 1. The material properties of FG nanoplate

Materials	Properties		
	E (Gpa)	$\rho(Kg/m^3)$	ν
SUS 304	201.04	8166	0.3
Si_3N_4	348.46	2370	0.3

Dimensionless natural frequency values are used in the present study for simply supported boundary conditions when the nanoplates are compared with obtained values by Aghababaei and Reddy [15] in table 2.

Table 2. Comparison of dimensionless frequency $\bar{\omega} = \omega h\sqrt{\rho/G}$ for a simply supported nanoplate with Aghababaei and Reddy

η	δ	μ	Present	[15]
1	10	0	0.0930	0.0935
1	10	1	0.0850	0.0854
1	10	2	0.0788	0.0791
1	20	0	0.0239	0.0239
1	20	1	0.0218	0.0218
1	20	2	0.0202	0.0202
2	10	0	0.0589	0.0591
2	10	1	0.0556	0.0557
2	10	2	0.0527	0.0529
2	20	0	0.0150	0.0150
2	20	1	0.0141	0.0141
2	20	2	0.0134	0.0134

The results show that deviation between our results and Aghababaei and Reddy's results is less than 1%.

In table 3, the dimensionless frequencies are compared with Ref [43] for simply supported and clamped FG nanoplates. As it is observed, the results obtained with the finite element method have considerable accuracy, as they are very close to the values obtained by reference.

The dimensionless frequencies of FG nanoplate for different nonlocal parameters, the power law index, and the mode number are listed in tables 4–8. Also, all combinations of simply supported and clamped boundary conditions are considered.

Table 3. Comparison of dimensionless frequency $\bar{\omega} = \omega h\sqrt{\rho_c/G_c}$ for FG square nanoplate $(\eta = 1, \delta = 0.1, n = 5)$

BC	Method	Dimensionless Frequency		
		$\mu = 0$	$\mu = 1$	$\mu = 2$
SSSS	Present	**0.0444**	**0.0405**	**0.0376**
	[43]	0.0441	0.0403	0.0374
CCCC	Present	**0.0753**	**0.0677**	**0.0620**
	[43]	0.0758	0.0682	0.0624

Table 4. Dimensionless frequency $\bar{\omega} = \omega h\sqrt{\rho_c/G_c}$ for FG SSSS square nanoplate $(\eta = 1, \delta = 0.1)$

Nonlocal parameter	Power law index	Dimensionless Frequency			
		Mode1	Mode 2	Mode 3	Mode 4
	$n = 0$				
$\mu = 0$		0.0930	0.2225	0.2225	0.3407
$\mu = 1$		0.0850	0.1820	0.1820	0.2547
$\mu = 2$		0.0788	0.1578	0.1578	0.2122
	$n = 1$				
$\mu = 0$		0.0552	0.1310	0.1310	0.2008
$\mu = 1$		0.0504	0.1072	0.1072	0.1501
$\mu = 2$		0.0467	0.0930	0.0930	0.1250
	$n = 5$				
$\mu = 0$		0.0444	0.1052	0.1052	0.1608
$\mu = 1$		0.0405	0.0861	0.0861	0.1202
$\mu = 2$		0.0376	0.0747	0.0747	0.1002

Table 5.Dimensionless frequency $\bar{\omega} = \omega h\sqrt{\rho_c / G_c}$ for FG SCSS square nanoplate $(\eta = 1, \delta = 0.1)$

Nonlocal parameter	Power law index	Dimensionless Frequency			
		Mode 1	Mode 2	Mode 3	Mode 4
	$n=0$				
$\mu=0$		0.1095	0.2305	0.2561	0.3627
$\mu=1$		0.0995	0.1881	0.2077	0.2695
$\mu=2$		0.0919	0.1629	0.1792	0.2239
	$n=1$				
$\mu=0$		0.0647	0.1357	0.1509	0.2137
$\mu=1$		0.0588	0.1108	0.1223	0.1588
$\mu=2$		0.0543	0.0959	0.1056	0.1319
	$n=5$				
$\mu=0$		0.0520	0.1089	0.1208	0.1708
$\mu=1$		0.0473	0.0889	0.0980	0.1270
$\mu=2$		0.0436	0.0770	0.0845	0.1055

Table 6. Dimensionless frequency $\bar{\omega} = \omega h\sqrt{\rho_c / G_c}$ for FG SCSC square nanoplate $(\eta = 1, \delta = 0.1)$

Nonlocal parameter	Power law index	Dimensionless Frequency			
		Mode 1	Mode 2	Mode 3	Mode 4
	$n=0$				
$\mu=0$		0.1307	0.2406	0.2921	0.3871
$\mu=1$		0.1185	0.1960	0.2350	0.2860
$\mu=2$		0.1092	0.1695	0.2018	0.2371
	$n=1$				
$\mu=0$		0.0771	0.1416	0.1722	0.2280
$\mu=1$		0.0699	0.1154	0.1384	0.1684
$\mu=2$		0.0644	0.0998	0.1189	0.1396
	$n=5$				
$\mu=0$		0.0618	0.1135	0.1373	0.1819
$\mu=1$		0.0560	0.0925	0.1105	0.1345
$\mu=2$		0.0516	0.0800	0.0949	0.1115

Table 7. Dimensionless frequency $\bar{\omega} = \omega h\sqrt{\rho_c / G_c}$ for FG SCCC square nanoplate $(\eta = 1, \delta = 0.1)$

Nonlocal parameter	Power law index	Dimensionless Frequency			
		Mode 1	Mode 2	Mode 3	Mode 4
	$n=0$				
$\mu=0$		0.1428	0.2719	0.2983	0.4066
$\mu=1$		0.1288	0.2195	0.2393	0.2985
$\mu=2$		0.1182	0.1889	0.2052	0.2468
	$n=1$				
$\mu=0$		0.0842	0.1602	0.1758	0.2395
$\mu=1$		0.0759	0.1292	0.1409	0.1758
$\mu=2$		0.0697	0.1112	0.1208	0.1453
	$n=5$				
$\mu=0$		0.0675	0.1280	0.1401	0.1908

Table 8. Dimensionless frequency $\bar{\omega} = \omega h\sqrt{\rho_c / G_c}$ for FG CCCC square nanoplate $(\eta = 1, \delta = 0.1)$

Nonlocal parameter	Power law index	Dimensionless Frequency			
		Mode 1	Mode 2	Mode 3	Mode 4
	$n=0$				
$\mu=0$		0.1597	0.3061	0.3061	0.4286
$\mu=1$		0.1436	0.2450	0.2450	0.3129
$\mu=2$		0.1315	0.2099	0.2099	0.2580
	$n=1$				
$\mu=0$		0.0941	0.1804	0.1804	0.2525
$\mu=1$		0.0846	0.1443	0.1443	0.1842
$\mu=2$		0.0774	0.1236	0.1236	0.1518
	$n=5$				
$\mu=0$		0.0753	0.1437	0.1437	02008
$\mu=1$		0.0677	0.1151	0.1151	0.1467
$\mu=2$		0.0620	0.0987	0.0987	0.1210

Figure 2 shows the changes of dimensionless frequency for an FG simply supported nanoplate based on the changes of nonlocal parameters for different power law index values. In this figure, it is observed that by increasing the nonlocal parameters and the power law index, non-dimensional frequency decreases. It is found that for the lower power law index, the value of dimensionless frequency is higher, because by increasing the power law index, the property of the plate reaches to metal, and so its stiffness decreases. Thus, for a higher power law index, the value of the dimensionless frequency is lower.

In figure 3, the effects of plate thickness on frequency ratio for different values of nonlocal parameters areshown. It is observed that by increasing plate thickness, there is no change in the frequency ratio.

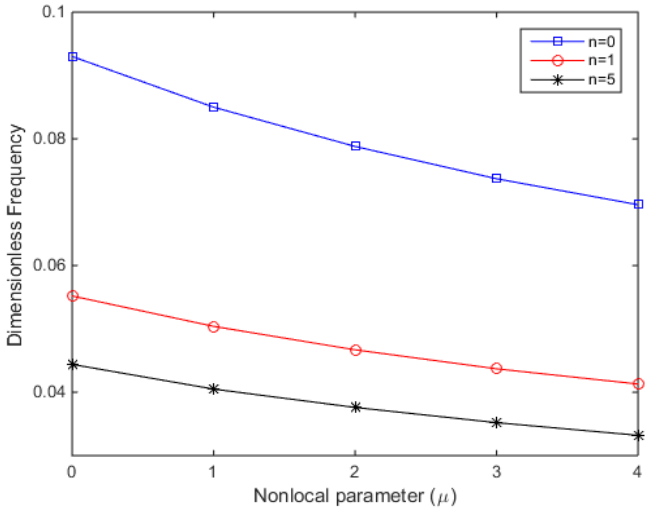

Figure 2. Effect of nonlocal parameter on dimensionless frequency for a FG simply supported nanoplate for different power law index $(\eta = 1, \delta = 0.1)$

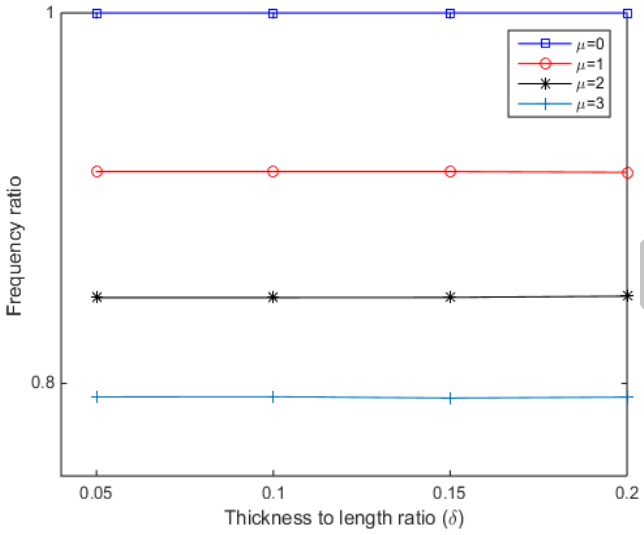

Figure 3. Effect of thickness to length ratio on frequency ratio for a FG simply supported nanoplate for different nonlocal parameters $(\eta = 1, n = 5)$

In figure 4, the effects of the aspect ratio on non-dimensional frequency for different values of nonlocal parameters are shown. It is observed that by increasing the aspect ratio, the frequency increases for all nonlocal parameters. It is clear that for the higher aspect ratios, the influence of the nonlocal parameters increases.

Figure 5 illustrates the effect of the nonlocal parameter on the frequency ratio for different modes of vibration for the clamped boundary condition. It is found that for higher mode numbers, the effect of the nonlocal parameter becomes more noticeable.

Figure 6 shows the effects of nonlocal parameters on the frequency ratio for different boundary conditions. It is found that size-dependent behavior is the greatest for the clamped boundary condition and the least for the simply supported boundary condition. Also, the size dependency increases by increasing the nonlocal parameter.

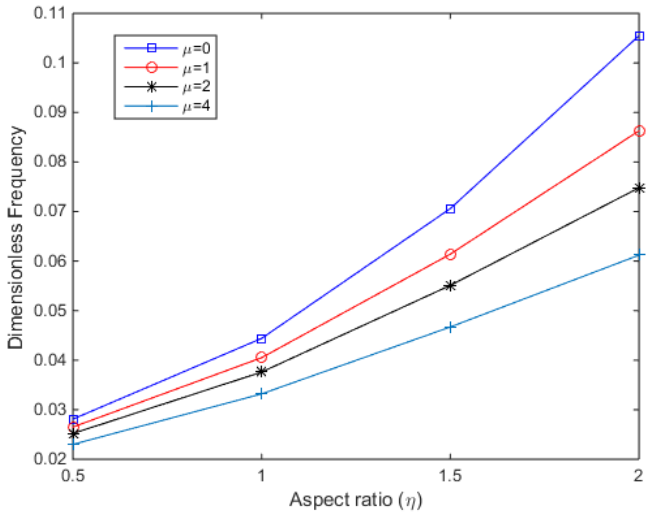

Figure 4. Effect of aspect ratio on dimensionless frequency for a FG simply supported nanoplate for different nonlocal parameters $(n = 5, \delta = 0.1)$

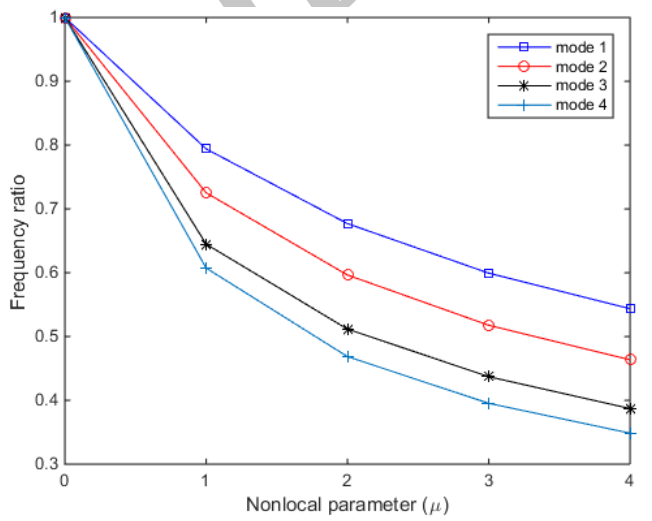

Figure 5 Effect of nonlocal parameter on frequency ratio for a FG clamped nanoplate for different mode numbers $(n = 5, \delta = 0.1, \eta = 2)$

Figure 7 shows the variation of dimensionless frequencies for FG nanoplates based on the changes of the power law index for different boundary conditions. It is obvious that by using stiffer boundary conditions at the edges, the dimensionless frequency will increase.

The variation of the dimensionless frequency of the FG clamped nanoplate with the power law index for different nonlocal parameters is shown in figure 8. This figure shows that increasing the power law index causes the dimensionless frequency to decrease for all nonlocal parameters. Also, by increasing the power law index, the dimensionless frequency converges to a specific value—the metallic plate frequency.

The effect of the aspect ratio on the frequency ratio for an FG nanoplate for different boundary conditions is shown in figure 9. It is clear that by increasing the aspect ratio of the plate, the frequency ratio decreases for all boundary conditions. Also, the effect of the aspect ratio is considerably more for the clamped boundary condition.

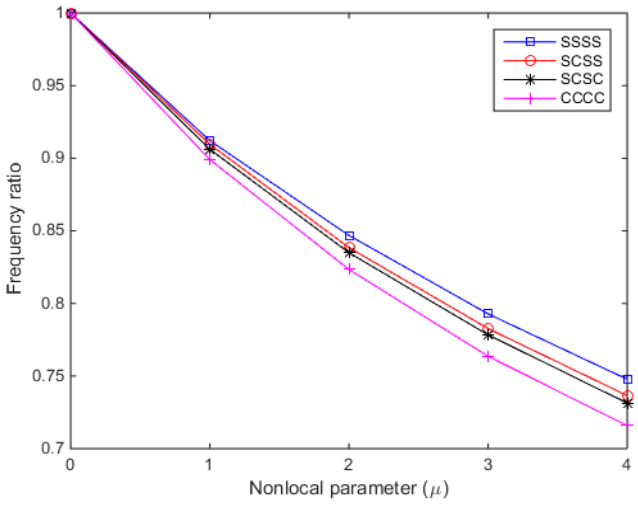

Figure 6 Effect of nonlocal parameter on frequency ratio for a FG square nanoplate for different boundary conditions $(n=5, \delta=0.1)$

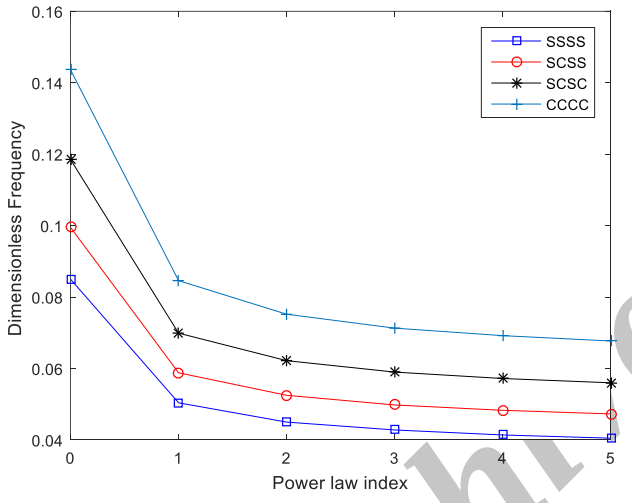

Figure 7 Effect of power law index on dimensionless frequency for a FG square nanoplate for different boundary conditions $(\delta=0.1, \mu=1)$

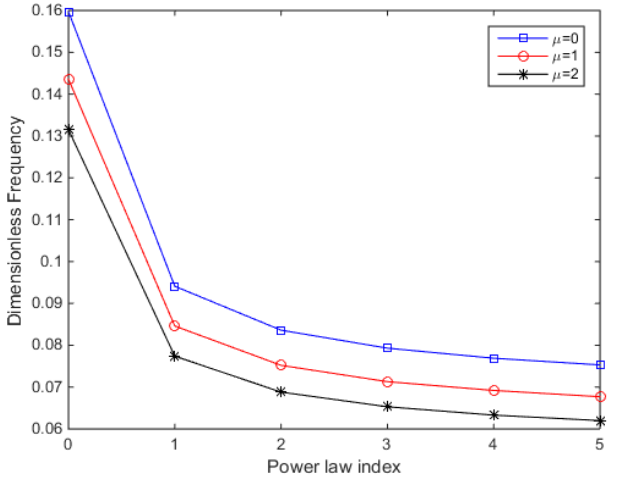

Figure 8. Effect of power law index on dimensionless frequency for a FG clamped nanoplate for different nonlocal parameters $(\delta=0.1, \eta=1)$

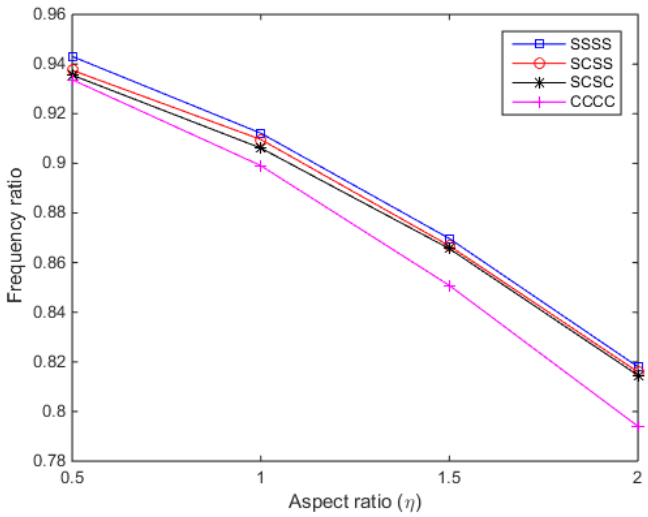

Figure 9 Effect of aspect ratio on frequency ratio for a FG nanoplate for different boundary conditions $(\delta=0.1, \mu=1, n=5)$

5. Conclusion

This paper presents an analysis of free vibration of FG nanoplate based on higher-order shear deformation plate theory using the finite element method. For implementing small-size effects, nonlocal theory is used. Dimensionless frequencies of the nanoplates are compared with the results of Aghababaei and Reddy's study, and the dimensionless frequencies for FG rectangular nanoplates are compared with available results by Ref [43];excellent agreement is observed. . In future works, these results can be an excellent database to verify approximate or analytical solutions. Also the influence of different parameters, such as nonlocal parameters, aspect ratio and aspect of length to thickness of nanoplate, are discussed. It was observed that:

- By increasing the nonlocal parameter and the power law index, non-dimensional frequency will decrease.
- By increasing the thickness of the nanoplate, there is no change in frequency ratio.
- By increasing the aspect ratio of the FG nanoplate, the frequency will increase for all nonlocal parameters.
- For higher mode numbers the effect of nonlocal parameter becomes more noticeable.
- The size-dependent behavior is the greatest for the clamped boundary condition and the least for the simply supported boundary condition
- By increasing the power law index, frequency will decrease for all boundary conditions.
- Dimensionless frequency increases by increasing the constraints at the edge.
- By increasing the aspect ratio of the FG nanoplate, the frequency ratio decreases for all boundary conditions.
- By increasing the power law index, the dimensionless frequency decreases for all nonlocal parameters.

6. Appendix A. Components of Finite Element Method Matrixes

Each component of stiffness and mass matrixes and force vector that have been discussed in solution method part are given below. The parameters that have been used in this matrixes are:

$$\begin{Bmatrix} a_0 \\ a_1 \\ a_2 \\ a_3 \\ a_4 \\ a_6 \end{Bmatrix} = \int_{-\frac{h}{2}}^{\frac{h}{2}} Q_{11} \begin{Bmatrix} 1 \\ z \\ z^2 \\ z^3 \\ z^4 \\ z^6 \end{Bmatrix} dz \tag{a1}$$

$$\begin{Bmatrix} b_0 \\ b_1 \\ b_2 \\ b_3 \\ b_4 \\ b_6 \end{Bmatrix} = \int_{-\frac{h}{2}}^{\frac{h}{2}} Q_{22} \begin{Bmatrix} 1 \\ z \\ z^2 \\ z^3 \\ z^4 \\ z^6 \end{Bmatrix} dz \tag{a2}$$

$$\begin{Bmatrix} d_0 \\ d_1 \\ d_2 \\ d_3 \\ d_4 \\ d_6 \end{Bmatrix} = \int_{-\frac{h}{2}}^{\frac{h}{2}} Q_{22} \begin{Bmatrix} 1 \\ z \\ z^2 \\ z^3 \\ z^4 \\ z^6 \end{Bmatrix} dz \tag{a3}$$

Where

$$Q_{11} = Q_{22} = \frac{E}{1-\nu^2} \tag{a4}$$

$$Q_{12} = Q_{21} = \frac{E\nu}{1-\nu^2} \tag{a5}$$

$$Q_{66} = \frac{E}{2(1+\nu)} \tag{a6}$$

Then the each component of the Matrixes and vector are

$$k_{11}^{ij} = \int_{\Omega_e} \left(a_0 \frac{\partial \psi_i^{(1)}}{\partial x} \frac{\partial \psi_j^{(1)}}{\partial x} + d_0 \frac{\partial \psi_i^{(1)}}{\partial y} \frac{\partial \psi_j^{(1)}}{\partial y} \right) dxdy \tag{a7}$$

$$k_{12}^{ij} = \int_{\Omega_e} \left(b_0 \frac{\partial \psi_i^{(1)}}{\partial x} \frac{\partial \psi_j^{(1)}}{\partial y} + d_0 \frac{\partial \psi_i^{(1)}}{\partial y} \frac{\partial \psi_j^{(1)}}{\partial x} \right) dxdy \tag{a8}$$

$$k_{13}^{ij} = \int_{\Omega_e} -c_1 \left(a_3 \frac{\partial \psi_i^{(1)}}{\partial x} \frac{\partial^2 \psi_j^{(2)}}{\partial x^2} + b_3 \frac{\partial \psi_i^{(1)}}{\partial x} \frac{\partial^2 \psi_j^{(2)}}{\partial y^2} + 2d_3 \frac{\partial \psi_i^{(1)}}{\partial x} \frac{\partial^2 \psi_j^{(2)}}{\partial x \partial y} \right) dxdy \tag{a9}$$

$$k_{14}^{ij} = \int_{\Omega_e} \left[(a_1 - c_1 a_3) \frac{\partial \psi_i^{(1)}}{\partial x} \frac{\partial \psi_j^{(3)}}{\partial x} + (d_1 - c_3 d_3) \frac{\partial \psi_i^{(1)}}{\partial y} \frac{\partial \psi_j^{(3)}}{\partial y} \right] dxdy \tag{a10}$$

$$k_{15}^{ij} = \int_{\Omega_e} \left[(b_1 - c_1 b_3) \frac{\partial \psi_i^{(1)}}{\partial x} \frac{\partial \psi_j^{(3)}}{\partial y} + (d_1 - c_3 d_3) \frac{\partial \psi_i^{(1)}}{\partial y} \frac{\partial \psi_j^{(3)}}{\partial x} \right] dxdy \tag{a11}$$

$$k_{21}^{ij} = \int_{\Omega_e} \left(b_0 \frac{\partial \psi_i^{(1)}}{\partial y} \frac{\partial \psi_j^{(1)}}{\partial x} + d_0 \frac{\partial \psi_i^{(1)}}{\partial x} \frac{\partial \psi_j^{(1)}}{\partial y} \right) dxdy \tag{a12}$$

$$k_{22}^{ij} = \int_{\Omega_e} \left(a_0 \frac{\partial \psi_i^{(1)}}{\partial y} \frac{\partial \psi_j^{(1)}}{\partial y} + d_0 \frac{\partial \psi_i^{(1)}}{\partial x} \frac{\partial \psi_j^{(1)}}{\partial x} \right) dxdy \tag{a13}$$

$$k_{23}^{ij}=\int_{\Omega_e}-c_1\left(a_3\frac{\partial\psi_i^{(1)}}{\partial y}\frac{\partial^2\psi_j^{(2)}}{\partial y^2}+b_3\frac{\partial\psi_i^{(1)}}{\partial y}\frac{\partial^2\psi_j^{(2)}}{\partial x^2}+2d_3\frac{\partial\psi_i^{(1)}}{\partial y}\frac{\partial^2\psi_j^{(2)}}{\partial x\partial y}\right)dxdy \tag{a14}$$

$$k_{24}^{ij}=\int_{\Omega_e}\left[\left(b_1-c_1b_3\right)\frac{\partial\psi_i^{(1)}}{\partial y}\frac{\partial\psi_j^{(3)}}{\partial x}+\left(d_1-c_3d_3\right)\frac{\partial\psi_i^{(1)}}{\partial x}\frac{\partial\psi_j^{(3)}}{\partial y}\right]dxdy \tag{a15}$$

$$k_{25}^{ij}=\int_{\Omega_e}\left[\left(a_1-c_1a_3\right)\frac{\partial\psi_i^{(1)}}{\partial y}\frac{\partial\psi_j^{(3)}}{\partial y}+\left(d_1-c_3d_3\right)\frac{\partial\psi_i^{(1)}}{\partial x}\frac{\partial\psi_j^{(3)}}{\partial x}\right]dxdy \tag{a16}$$

$$k_{31}^{ij}=\int_{\Omega_e}-c_1\left(a_3\frac{\partial^2\psi_i^{(2)}}{\partial x^2}\frac{\partial\psi_j^{(1)}}{\partial x}+b_3\frac{\partial^2\psi_i^{(2)}}{\partial y^2}\frac{\partial\psi_j^{(1)}}{\partial x}+2d_3\frac{\partial^2\psi_i^{(2)}}{\partial x\partial y}\frac{\partial\psi_j^{(1)}}{\partial y}\right)dxdy \tag{a17}$$

$$k_{32}^{ij}=\int_{\Omega_e}-c_1\left(b_3\frac{\partial^2\psi_i^{(2)}}{\partial x^2}\frac{\partial\psi_j^{(1)}}{\partial y}+a_3\frac{\partial^2\psi_i^{(2)}}{\partial y^2}\frac{\partial\psi_j^{(1)}}{\partial y}+2d_3\frac{\partial^2\psi_i^{(2)}}{\partial x\partial y}\frac{\partial\psi_j^{(1)}}{\partial x}\right)dxdy \tag{a18}$$

$$k_{33}^{ij}=\int_{\Omega_e}\left[\begin{array}{l}c_1^{\,2}\left(a_6\left(\frac{\partial^2\psi_i^{(2)}}{\partial x^2}\frac{\partial^2\psi_j^{(2)}}{\partial x^2}+\frac{\partial^2\psi_i^{(2)}}{\partial y^2}\frac{\partial^2\psi_j^{(2)}}{\partial y^2}\right)+b_6\left(\frac{\partial^2\psi_i^{(2)}}{\partial x^2}\frac{\partial^2\psi_j^{(2)}}{\partial y^2}+\frac{\partial^2\psi_i^{(2)}}{\partial y^2}\frac{\partial^2\psi_j^{(2)}}{\partial x^2}\right)+4d_6\frac{\partial^2\psi_i^{(2)}}{\partial x\partial y}\frac{\partial^2\psi_j^{(2)}}{\partial x\partial y}\right)\\+\left(d_0-2c_2d_2+c_2^{\,2}d_4\right)\left(\frac{\partial\psi_i^{(2)}}{\partial x}\frac{\partial\psi_j^{(2)}}{\partial x}+\frac{\partial\psi_i^{(2)}}{\partial y}\frac{\partial\psi_j^{(2)}}{\partial y}\right)\end{array}\right]dxdy \tag{a19}$$

$$k_{34}^{ij}=\int_{\Omega_e}\left[\begin{array}{l}\left(-c_1a_4+c_1^{\,2}a_6\right)\frac{\partial^2\psi_i^{(2)}}{\partial x^2}\frac{\partial\psi_j^{(3)}}{\partial x}+\left(-c_1b_4+c_1^{\,2}b_6\right)\frac{\partial^2\psi_i^{(2)}}{\partial y^2}\frac{\partial\psi_j^{(3)}}{\partial x}\\+2\left(-c_1d_4+c_1^{\,2}d_6\right)\frac{\partial^2\psi_i^{(2)}}{\partial x\partial y}\frac{\partial\psi_j^{(3)}}{\partial y}+\left(d_0-2c_2d_2+c_2^{\,2}d_4\right)\frac{\partial\psi_i^{(2)}}{\partial x}\psi_j^{(3)}\end{array}\right]dxdy \tag{a20}$$

$$k_{35}^{ij}=\int_{\Omega_e}\left[\begin{array}{l}\left(-c_1a_4+c_1^{\,2}a_6\right)\frac{\partial^2\psi_i^{(2)}}{\partial y^2}\frac{\partial\psi_j^{(3)}}{\partial y}+\left(-c_1b_4+c_1^{\,2}b_6\right)\frac{\partial^2\psi_i^{(2)}}{\partial x^2}\frac{\partial\psi_j^{(3)}}{\partial y}\\+2\left(-c_1d_4+c_1^{\,2}d_6\right)\frac{\partial^2\psi_i^{(2)}}{\partial x\partial y}\frac{\partial\psi_j^{(3)}}{\partial x}+\left(d_0-2c_2d_2+c_2^{\,2}d_4\right)\frac{\partial\psi_i^{(2)}}{\partial y}\psi_j^{(3)}\end{array}\right]dxdy \tag{a21}$$

$$k_{41}^{ij}=\int_{\Omega_e}\left[\left(a_1-c_1a_3\right)\frac{\partial\psi_i^{(3)}}{\partial x}\frac{\partial\psi_j^{(1)}}{\partial x}+\left(d_1-c_1d_3\right)\frac{\partial\psi_i^{(3)}}{\partial y}\frac{\partial\psi_j^{(1)}}{\partial y}\right]dxdy \tag{a22}$$

$$k_{42}^{ij}=\int_{\Omega_e}\left[\left(b_1-c_1b_3\right)\frac{\partial\psi_i^{(3)}}{\partial x}\frac{\partial\psi_j^{(1)}}{\partial y}+\left(d_1-c_1d_3\right)\frac{\partial\psi_i^{(3)}}{\partial y}\frac{\partial\psi_j^{(1)}}{\partial x}\right]dxdy \tag{a23}$$

$$k_{43}^{ij}=\int_{\Omega_e}\left[\begin{array}{l}\left(-c_1a_4+c_1^{\,2}a_6\right)\frac{\partial\psi_i^{(3)}}{\partial x}\frac{\partial^2\psi_j^{(2)}}{\partial x^2}+\left(-c_1b_4+c_1^{\,2}b_6\right)\frac{\partial\psi_i^{(3)}}{\partial x}\frac{\partial^2\psi_j^{(2)}}{\partial y^2}\\+2\left(-c_1d_4+c_1^{\,2}d_6\right)\frac{\partial\psi_i^{(3)}}{\partial y}\frac{\partial^2\psi_j^{(2)}}{\partial x\partial y}+\left(d_0-2c_2d_2+c_2^{\,2}d_4\right)\psi_i^{(3)}\frac{\partial\psi_j^{(2)}}{\partial x}\end{array}\right]dxdy \tag{a24}$$

$$k_{44}^{ij}=\int_{\Omega_e}\left[\begin{array}{l}\left(a_2-2c_1a_4+{c_1}^2a_6\right)\dfrac{\partial\psi_i^{(3)}}{\partial x}\dfrac{\partial\psi_j^{(3)}}{\partial x}+\left(d_2-2c_1d_4+{c_1}^2d_6\right)\dfrac{\partial\psi_i^{(3)}}{\partial y}\dfrac{\partial\psi_j^{(3)}}{\partial y}\\+\left(d_0-2c_2d_2+{c_2}^2d_4\right)\psi_i^{(3)}\psi_j^{(3)}\end{array}\right]dxdy \tag{a25}$$

$$k_{45}^{ij}=\int_{\Omega_e}\left[\left(b_2-2c_1b_4+{c_1}^2b_6\right)\frac{\partial\psi_i^{(3)}}{\partial x}\frac{\partial\psi_j^{(3)}}{\partial y}+\left(d_2-2c_1d_4+{c_1}^2d_6\right)\frac{\partial\psi_i^{(3)}}{\partial y}\frac{\partial\psi_j^{(3)}}{\partial x}\right]dxdy \tag{a26}$$

$$k_{51}^{ij}=\int_{\Omega_e}\left[\left(b_1-c_1b_3\right)\frac{\partial\psi_i^{(3)}}{\partial y}\frac{\partial\psi_j^{(1)}}{\partial x}+\left(d_1-c_3d_3\right)\frac{\partial\psi_i^{(3)}}{\partial x}\frac{\partial\psi_j^{(1)}}{\partial y}\right]dxdy \tag{a27}$$

$$k_{52}^{ij}=\int_{\Omega_e}\left[\left(a_1-c_1a_3\right)\frac{\partial\psi_i^{(3)}}{\partial y}\frac{\partial\psi_j^{(1)}}{\partial y}+\left(d_1-c_3d_3\right)\frac{\partial\psi_j^{(3)}}{\partial x}\frac{\partial\psi_j^{(1)}}{\partial x}\right]dxdy \tag{a28}$$

$$k_{53}^{ij}=\int_{\Omega_e}\left[\begin{array}{l}\left(-c_1a_4+{c_1}^2a_6\right)\dfrac{\partial\psi_i^{(3)}}{\partial y}\dfrac{\partial^2\psi_j^{(2)}}{\partial y^2}+\left(-c_1b_4+{c_1}^2b_6\right)\dfrac{\partial\psi_i^{(3)}}{\partial y}\dfrac{\partial^2\psi_j^{(2)}}{\partial x^2}\\+2\left(-c_1d_4+{c_1}^2d_6\right)\dfrac{\partial\psi_i^{(3)}}{\partial x}\dfrac{\partial^2\psi_j^{(2)}}{\partial x\partial y}+\left(d_0-2c_2d_2+{c_2}^2d_4\right)\psi_i^{(3)}\dfrac{\partial\psi_j^{(2)}}{\partial y}\end{array}\right]dxdy \tag{a29}$$

$$k_{54}^{ij}=\int_{\Omega_e}\left[\left(b_2-2c_1b_4+{c_1}^2b_6\right)\frac{\partial\psi_i^{(3)}}{\partial y}\frac{\partial\psi_j^{(3)}}{\partial x}+\left(d_2-2c_1d_4+{c_1}^2d_6\right)\frac{\partial\psi_i^{(3)}}{\partial x}\frac{\partial\psi_j^{(3)}}{\partial y}\right]dxdy \tag{a30}$$

$$k_{55}^{ij}=\int_{\Omega_e}\left[\begin{array}{l}\left(a_2-2c_1a_4+{c_1}^2a_6\right)\dfrac{\partial\psi_i^{(3)}}{\partial y}\dfrac{\partial\psi_j^{(3)}}{\partial y}+\left(d_2-2c_1d_4+{c_1}^2d_6\right)\dfrac{\partial\psi_i^{(3)}}{\partial x}\dfrac{\partial\psi_j^{(3)}}{\partial x}\\+\left(d_0-2c_2d_2+{c_2}^2d_4\right)\psi_i^{(3)}\psi_j^{(3)}\end{array}\right]dxdy \tag{a31}$$

$$m_{11}^{ij}=\int_{\Omega_e}m_0\left(\psi_i^{(1)}\psi_j^{(1)}+\mu\left(\frac{\partial\psi_i^{(1)}}{\partial x}\frac{\partial\psi_j^{(1)}}{\partial x}+\frac{\partial\psi_i^{(1)}}{\partial y}\frac{\partial\psi_j^{(1)}}{\partial y}\right)\right)dxdy \tag{a32}$$

$$m_{13}^{ij}=\int_{\Omega_e}-c_1m_3\left(\psi_i^{(1)}\frac{\partial\psi_j^{(2)}}{\partial x}+\mu\left(\frac{\partial\psi_i^{(1)}}{\partial x}\frac{\partial^2\psi_j^{(2)}}{\partial x^2}+\frac{\partial\psi_i^{(1)}}{\partial y}\frac{\partial^2\psi_j^{(2)}}{\partial x\partial y}\right)\right)dxdy \tag{a33}$$

$$m_{14}^{ij}=\int_{\Omega_e}\left(m_1-c_1m_3\right)\left(\psi_i^{(1)}\psi_j^{(3)}+\mu\left(\frac{\partial\psi_i^{(1)}}{\partial x}\frac{\partial\psi_j^{(3)}}{\partial x}+\frac{\partial\psi_i^{(1)}}{\partial y}\frac{\partial\psi_j^{(3)}}{\partial y}\right)\right)dxdy \tag{a34}$$

$$m_{22}^{ij}=\int_{\Omega_e}m_0\left(\psi_i^{(1)}\psi_j^{(1)}+\mu\left(\frac{\partial\psi_i^{(1)}}{\partial x}\frac{\partial\psi_j^{(1)}}{\partial x}+\frac{\partial\psi_i^{(1)}}{\partial y}\frac{\partial\psi_j^{(1)}}{\partial y}\right)\right)dxdy \tag{a35}$$

$$m_{23}^{ij}=\int_{\Omega_e}-c_1m_3\left(\psi_i^{(1)}\frac{\partial\psi_j^{(2)}}{\partial y}+\mu\left(\frac{\partial\psi_i^{(1)}}{\partial x}\frac{\partial^2\psi_j^{(2)}}{\partial x\partial y}+\frac{\partial\psi_i^{(1)}}{\partial y}\frac{\partial^2\psi_j^{(2)}}{\partial y^2}\right)\right)dxdy \tag{a36}$$

$$m_{25}^{ij}=\int_{\Omega_e}\left(m_1-c_1m_3\right)\left(\psi_i^{(1)}\psi_j^{(3)}+\mu\left(\frac{\partial\psi_i^{(1)}}{\partial x}\frac{\partial\psi_j^{(3)}}{\partial x}+\frac{\partial\psi_i^{(1)}}{\partial y}\frac{\partial\psi_j^{(3)}}{\partial y}\right)\right)dxdy \tag{a37}$$

$$m_{33}^{ij}=\int_{\Omega_e}\left[\begin{array}{l} m_0\left(\psi_i^{(3)}\psi_j^{(3)}+\mu\left(\frac{\partial\psi_i^{(3)}}{\partial x}\frac{\partial\psi_j^{(3)}}{\partial x}+\frac{\partial\psi_i^{(3)}}{\partial y}\frac{\partial\psi_j^{(3)}}{\partial y}\right)\right) \\ +c_1{}^2m_6\left(\frac{\partial\psi_i^{(3)}}{\partial x}\frac{\partial\psi_j^{(3)}}{\partial x}+\mu\left(\frac{\partial^2\psi_i^{(3)}}{\partial x^2}\frac{\partial^2\psi_j^{(3)}}{\partial x^2}+\frac{\partial^2\psi_i^{(3)}}{\partial x\partial y}\frac{\partial^2\psi_j^{(3)}}{\partial x\partial y}\right)\right) \\ +c_1{}^2m_6\left(\frac{\partial\psi_i^{(3)}}{\partial y}\frac{\partial\psi_j^{(3)}}{\partial y}+\mu\left(\frac{\partial^2\psi_i^{(3)}}{\partial x\partial y}\frac{\partial^2\psi_j^{(3)}}{\partial x\partial y}+\frac{\partial^2\psi_i^{(3)}}{\partial y^2}\frac{\partial^2\psi_j^{(3)}}{\partial y^2}\right)\right) \end{array}\right]dxdy \tag{a38}$$

$$m_{43}^{ij}=\int_{\Omega_e}\left(-c_1m_4+c_1{}^2m_6\right)\left(\psi_i^{(3)}\frac{\partial\psi_j^{(2)}}{\partial x}+\mu\left(\frac{\partial\psi_i^{(3)}}{\partial x}\frac{\partial^2\psi_j^{(2)}}{\partial x^2}+\frac{\partial\psi_i^{(3)}}{\partial y}\frac{\partial^2\psi_j^{(2)}}{\partial x\partial y}\right)\right)dxdy \tag{a39}$$

$$m_{44}^{ij}=\int_{\Omega_e}\left(m_2-2c_1m_4+m_6\right)\left(\psi_i^{(3)}\psi_j^{(3)}+\mu\left(\frac{\partial\psi_i^{(3)}}{\partial x}\frac{\partial\psi_j^{(3)}}{\partial x}+\frac{\partial\psi_i^{(3)}}{\partial y}\frac{\partial\psi_j^{(3)}}{\partial y}\right)\right)dxdy \tag{a40}$$

$$m_{53}^{ij}=\int_{\Omega_e}\left(-c_1m_4+c_1{}^2m_6\right)\left(\psi_i^{(3)}\frac{\partial\psi_j^{(2)}}{\partial y}+\mu\left(\frac{\partial\psi_i^{(3)}}{\partial x}\frac{\partial^2\psi_j^{(2)}}{\partial x\partial y}+\frac{\partial\psi_i^{(3)}}{\partial y}\frac{\partial^2\psi_j^{(2)}}{\partial y^2}\right)\right)dxdy \tag{a41}$$

$$m_{55}^{ij}=\int_{\Omega_e}\left(m_2-2c_1m_4+m_6\right)\left(\psi_i^{(3)}\psi_j^{(3)}+\mu\left(\frac{\partial\psi_i^{(3)}}{\partial x}\frac{\partial\psi_j^{(3)}}{\partial x}+\frac{\partial\psi_i^{(3)}}{\partial y}\frac{\partial\psi_j^{(3)}}{\partial y}\right)\right)dxdy \tag{a42}$$

References

[1] T. Aksencer, M. Aydogdu, Levy type solution method for vibration and buckling of nanoplates using nonlocal elasticity theory, *Physica E: Low-dimensional Systems and Nanostructures*, Vol. 43, No. 4, pp. 954-959, 2011.

[2] R. Ansari, R. Rajabiehfard, B. Arash, Nonlocal finite element model for vibrations of embedded multi-layered graphene sheets, *Computational Materials Science*, Vol. 49, No. 4, pp. 831-838, 2010.

[3] S. H. Hashemi, A. T. Samaei, Buckling analysis of micro/nanoscale plates via nonlocal elasticity theory, *Physica E: Low-dimensional Systems and Nanostructures*, Vol. 43, No. 7, pp. 1400-1404, 2011.

[4] S. Narendar, Buckling analysis of micro-/nano-scale plates based on two-variable refined plate theory incorporating nonlocal scale effects, *Composite Structures*, Vol. 93, No. 12, pp. 3093-3103, 2011.

[5] A. Daneshmehr, A. Rajabpoor, A. Hadi, Size dependent free vibration analysis of nanoplates made of functionally graded materials based on nonlocal elasticity theory with high order theories, *International Journal of Engineering Science*, Vol. 95, pp. 23-35, 2015.

[6] A. BAKHSHESHY, K. KHORSHIDI, Free Vibration of Functionally Graded Rectangular Nanoplates in Thermal Environment Based on the Modified Couple Stress Theory, 2015.

[7] S. Hosseini-Hashemi, H. R. D. Taher, H. Akhavan, M. Omidi, Free vibration of functionally graded rectangular plates using first-order shear deformation plate theory, *Applied Mathematical Modelling*, Vol. 34, No. 5, pp. 1276-1291, 2010.

[8] M. Zare, R. Nazemnezhad, S. Hosseini-Hashemi, Natural frequency analysis of functionally graded rectangular nanoplates with different boundary conditions via an analytical method, *Meccanica*, Vol. 50, No. 9, pp. 2391-2408, 2015.

[9] F. Bounouara, K. H. Benrahou, I. Belkorissat, A. Tounsi, A nonlocal zeroth-order shear deformation theory for free vibration of functionally graded nanoscale plates resting on elastic foundation, *Steel and Composite Structures*, Vol. 20, No. 2, pp. 227-249, 2016.

[10] H. Salehipour, H. Nahvi, A. Shahidi, Exact closed-form free vibration analysis for functionally graded micro/nano plates based on modified couple stress and three-dimensional elasticity theories, *Composite Structures*, Vol. 124, pp. 283-291, 2015.

[11] I. Belkorissat, M. S. A. Houari, A. Tounsi, E. Bedia, S.

Mahmoud, On vibration properties of functionally graded nano-plate using a new nonlocal refined four variable model, *Steel and Composite Structures*, Vol. 18, No. 4, pp. 1063-1081, 2015.

[12] R. Ansari, M. Ashrafi, T. Pourashraf, S. Sahmani, Vibration and buckling characteristics of functionally graded nanoplates subjected to thermal loading based on surface elasticity theory, *Acta Astronautica*, Vol. 109, pp. 42-51, 2015.

[13] M. Hosseini, A. Jamalpoor, Analytical solution for thermomechanical vibration of double-viscoelastic nanoplate-systems made of functionally graded materials, *Journal of Thermal Stresses*, Vol. 38, No. 12, pp. 1428-1456, 2015.

[14] R. Ansari, M. F. Shojaei, A. Shahabodini, M. Bazdid-Vahdati, Three-dimensional bending and vibration analysis of functionally graded nanoplates by a novel differential quadrature-based approach, *Composite Structures*, Vol. 131, pp. 753-764, 2015.

[15] R. Aghababaei, J. Reddy, Nonlocal third-order shear deformation plate theory with application to bending and vibration of plates, *Journal of Sound and Vibration*, Vol. 326, No. 1, pp. 277-289, 2009.

[16] R. B. Bouiadjra, E. Bedia, A. Tounsi, Nonlinear thermal buckling behavior of functionally graded plates using an efficient sinusoidal shear deformation theory, *Structural Engineering and Mechanics*, Vol. 48, No. 4, pp. 547-567, 2013.

[17] N.-T. Nguyen, D. Hui, J. Lee, H. Nguyen-Xuan, An efficient computational approach for size-dependent analysis of functionally graded nanoplates, *Computer Methods in Applied Mechanics and Engineering*, Vol. 297, pp. 191-218, 2015.

[18] A. Daneshmehr, A. Rajabpoor, Stability of size dependent functionally graded nanoplate based on nonlocal elasticity and higher order plate theories and different boundary conditions, *International Journal of Engineering Science*, Vol. 82, pp. 84-100, 2014.

[19] A. Ghorbanpour Arani, H. Baba Akbar Zarei, E. Haghparast, Application of Halpin-Tsai Method in Modelling and Size-dependent Vibration Analysis of CNTs/fiber/polymer Composite Microplates, *Journal of Computational Applied Mechanics*, Vol. 47, No. 1, pp. 45-52, 2016.

[20] M. Goodarzi, M. N. Bahrami, V. Tavaf, Refined plate theory for free vibration analysis of FG nanoplates using the nonlocal continuum plate model, *Journal of Computational Applied Mechanics*, Vol. 48, No. 1, pp. 123-136, 2017.

[21] H. Raissi, M. Shishehsaz, S. Moradi, Applications of higher order shear deformation theories on stress distribution in a five layer sandwich plate.

[22] M. H. Ghayesh, H. Farokhi, A. Gholipour, M. Tavallaeinejad, Nonlinear oscillations of functionally graded microplates, *International Journal of Engineering Science*, Vol. 122, pp. 56-72, 2018.

[23] M. Baghani, M. Mohammadi, A. Farajpour, Dynamic and stability analysis of the rotating nanobeam in a nonuniform magnetic field considering the surface energy, *International Journal of Applied Mechanics*, Vol. 8, No. 04, pp. 1650048, 2016.

[24] M. H. Ghayesh, H. Farokhi, A. Gholipour, Oscillations of functionally graded microbeams, *International Journal of Engineering Science*, Vol. 110, pp. 35-53, 2017.

[25] N. Kordani, A. Fereidoon, M. Divsalar, A. Farajpour, Influence of surface piezoelectricity on the forced vibration of piezoelectric nanowires based on nonlocal elasticity theory, *Journal of Computational Applied Mechanics*, Vol. 47, No. 2, pp. 137-150, 2016.

[26] A. Farajpour, A. Rastgoo, Influence of carbon nanotubes on the buckling of microtubule bundles in viscoelastic cytoplasm using nonlocal strain gradient theory, *Results in physics*, Vol. 7, pp. 1367-1375, 2017.

[27] M. Hosseini, H. H. Gorgani, M. Shishesaz, A. Hadi, Size-Dependent Stress Analysis of Single-Wall Carbon Nanotube Based on Strain Gradient Theory, *International Journal of Applied Mechanics*, Vol. 9, No. 06, pp. 1750087, 2017.

[28] M. Hosseini, M. Shishesaz, K. N. Tahan, A. Hadi, Stress analysis of rotating nano-disks of variable thickness made of functionally graded materials, *International Journal of Engineering Science*, Vol. 109, pp. 29-53, 2016.

[29] M. Z. Nejad, A. Rastgoo, A. Hadi, Effect of exponentially-varying properties on displacements and stresses in pressurized functionally graded thick spherical shells with using iterative technique, *Journal of Solid Mechanics*, Vol. 6, No. 4, pp. 366-377, 2014.

[30] M. Z. Nejad, A. Hadi, Eringen's non-local elasticity theory for bending analysis of bi-directional functionally graded Euler–Bernoulli nano-beams, *International Journal of Engineering Science*, Vol. 106, pp. 1-9, 2016.

[31] M. Z. Nejad, A. Hadi, Non-local analysis of free vibration of bi-directional functionally graded Euler–Bernoulli nano-beams, *International Journal of Engineering Science*, Vol. 105, pp. 1-11, 2016.

[32] M. Z. Nejad, A. Hadi, A. Farajpour, Consistent couple-stress theory for free vibration analysis of Euler-Bernoulli nano-beams made of arbitrary bi-directional functionally graded materials, *Structural Engineering and Mechanics*, Vol. 63, No. 2, pp. 161-169, 2017.

[33] M. Z. Nejad, A. Hadi, A. Rastgoo, Buckling analysis of arbitrary two-directional functionally graded Euler–Bernoulli nano-beams based on nonlocal elasticity theory, *International Journal of Engineering Science*, Vol. 103, pp. 1-10, 2016.

[34] M. Z. Nejad, A. Rastgoo, A. Hadi, Exact elasto-plastic analysis of rotating disks made of functionally graded materials, *International Journal of Engineering Science*, Vol. 85, pp. 47-57, 2014.

[35] M. Shishesaz, M. Hosseini, K. N. Tahan, A. Hadi, Analysis of functionally graded nanodisks under thermoelastic loading based on the strain gradient theory, *Acta Mechanica*, Vol. 228, No. 12, pp. 4141-4168, 2017.

[36] A. Hadi, M. Z. Nejad, A. Rastgoo, M. Hosseini, Buckling analysis of FGM Euler-Bernoulli nano-beams with 3D-varying properties based on consistent couple-stress theory, *Steel and Composite Structures*, Vol. 26, No. 6, pp. 663-672, 2018.

[37] M. Zamani Nejad, M. Jabbari, A. Hadi, A review of functionally graded thick cylindrical and conical shells, *Journal of Computational Applied Mechanics*, Vol. 48,

No. 2, pp. 357-370, 2017.

[38] A. Hadi, M. Z. Nejad, M. Hosseini, Vibrations of three-dimensionally graded nanobeams, *International Journal of Engineering Science*, Vol. 128, pp. 12-23, 2018.

[39] J. N. Reddy, A simple higher-order theory for laminated composite plates, *Journal of applied mechanics*, Vol. 51, No. 4, pp. 745-752, 1984.

[40] H.-S. Shen, Nonlinear bending response of functionally graded plates subjected to transverse loads and in thermal environments, *International Journal of Mechanical Sciences*, Vol. 44, No. 3, pp. 561-584, 2002.

[41] A. C. Eringen, 2002, *Nonlocal continuum field theories*, Springer Science & Business Media,

[42] S. Tajalli, M. M. Zand, M. Ahmadian, Effect of geometric nonlinearity on dynamic pull-in behavior of coupled-domain microstructures based on classical and shear deformation plate theories, *European Journal of Mechanics-A/Solids*, Vol. 28, No. 5, pp. 916-925, 2009.

[43] S. Natarajan, S. Chakraborty, M. Thangavel, S. Bordas, T. Rabczuk, Size-dependent free flexural vibration behavior of functionally graded nanoplates, *Computational Materials Science*, Vol. 65, pp. 74-80, 2012.